Locating primary somatosensory cortex in human brain stimulation studies: experimental evidence

Article

It is advisable to refer to the publisher's version if you intend to cite from the work. See Guidance on citing.

To link to this article DOI: http://dx.doi.org/10.1152/jn.00641.2018

www.reading.ac.uk/centaur

RESEARCH ARTICLE | *Sensory Processing*

Locating primary somatosensory cortex in human brain stimulation studies: experimental evidence

 Nicholas Paul Holmes,[1] Luigi Tamè,[2] Paisley Beeching,[1] Mary Medford,[3] Mariyana Rakova,[3] Alexander Stuart,[1] and Silvia Zeni[1]

[1]*School of Psychology, University of Nottingham, University Park, Nottingham, United Kingdom;* [2]*Department of Psychological Sciences, Birkbeck University of London, London, United Kingdom; and* [3]*School of Psychology and Clinical Language Sciences, University of Reading, Reading, United Kingdom*

Holmes NP, Tamè L, Beeching P, Medford M, Rakova M, Stuart A, Zeni S. Locating primary somatosensory cortex in human brain stimulation studies: experimental evidence. *J Neurophysiol* 121: 336–344, 2019. First published December 21, 2018; doi:10.1152/jn.00641.2018.—Transcranial magnetic stimulation (TMS) over human primary somatosensory cortex (S1) does not produce immediate outputs. Researchers must therefore rely on indirect methods for TMS coil positioning. The "gold standard" is to use individual functional and structural magnetic resonance imaging (MRI) data, but the majority of studies don't do this. The most common method to locate the hand area of S1 (S1-hand) is to move the coil posteriorly from the hand area of primary motor cortex (M1-hand). Yet, S1-hand is not directly posterior to M1-hand. We localized the index finger area of S1-hand (S1-index) experimentally in four ways. First, we reanalyzed functional MRI data from 20 participants who received vibrotactile stimulation to their 10 digits. Second, to assist the localization of S1-hand without MRI data, we constructed a probabilistic atlas of the central sulcus from 100 healthy adult MRIs and measured the likely scalp location of S1-index. Third, we conducted two experiments mapping the effects of TMS across the scalp on tactile discrimination performance. Fourth, we examined all available neuronavigation data from our laboratory on the scalp location of S1-index. Contrary to the prevailing method, and consistent with systematic review evidence, S1-index is close to the C3/C4 electroencephalography (EEG) electrode locations on the scalp, ~7–8 cm lateral to the vertex, and ~2 cm lateral and 0.5 cm posterior to the M1-hand scalp location. These results suggest that an immediate revision to the most commonly used heuristic to locate S1-hand is required. The results of many TMS studies of S1-hand need reassessment.

NEW & NOTEWORTHY Noninvasive human brain stimulation requires indirect methods to target particular brain areas. Magnetic stimulation studies of human primary somatosensory cortex have used scalp-based heuristics to find the target, typically locating it 2 cm posterior to the motor cortex. We measured the scalp location of the hand area of primary somatosensory cortex and found that it is ~2 cm lateral to motor cortex. Our results suggest an immediate revision of the prevailing method is required.

S1; SI; TMS; TDCS; vibrotactile

Address for reprint requests and other correspondence: N. P. Holmes, School of Psychology, University of Nottingham, University Park, Nottingham, UK (e-mail: npholmes@neurobiography.info).

INTRODUCTION

Transcranial magnetic stimulation (TMS) (Barker et al. 1985) can be used to study the healthy human brain noninvasively, by stimulating brain tissue electromagnetically. TMS therefore requires indirect methods of locating the brain area of interest. Primary motor cortex (M1) can be located relatively easily, by moving the TMS coil around on the scalp, applying single pulses of TMS, and observing or recording muscle responses; however, for most other brain areas, there is no similar immediate and objective output that researchers can use, on a pulse-by-pulse basis, to ensure correct TMS coil position. The "gold standard" in this field is to acquire, for every participant, structural and functional brain imaging data and use frameless stereotaxy (Sparing et al. 2010).

When MRI is not available, researchers have used scalp-based heuristics to target the hand area of primary somatosensory cortex (S1-hand; Holmes and Tamè 2019). These heuristics have included using the 10-20 or 10-10 electroencephalographic system (Jasper 1958; Koessler et al. 2009; Lagerlund et al. 1993; Okamoto et al. 2004; Towle et al. 1993; Vitali et al. 2002; Xiao et al. 2018), functionally identified scalp locations for motor cortex (e.g., Balslev et al. 2004), changes in reaction times or errors (e.g., Convento et al. 2018), or changes in sensation (e.g., Cowey and Walsh 2000; Sugishita and Takayama 1993). Systematic review revealed the most common heuristic involves positioning the coil 2 cm posterior to the M1 representation of hand muscles (e.g., first dorsal interosseus, FDI, or abductor pollicis brevis, APB), yet S1-hand is lateral, not posterior to M1-hand (Holmes and Tamè 2019). In previous work using individual functional MRI (fMRI)-guided neuronavigation (Tamè and Holmes 2016), we noticed that, in all 20 of our participants, the scalp location above the index finger area of S1-hand (S1-index) was indeed lateral, not directly posterior, to M1.

Here, we ask "What is the optimal location on the scalp to magnetically stimulate the somatosensory cortex (Brodmann's areas BA3b and BA1; Geyer et al. 1999) representations of the index finger (S1-index)?" The index finger and the FDI muscles are the most commonly stimulated and recorded body parts, respectively, in the relevant literature, so we focused on them. We focused on the BA3b and BA1 subregions of S1 because they show a clear somatotopy for individual fingers

(Nelson and Chen 2008), because our fMRI protocol was not able to distinguish between them, and, for the purposes of applying TMS on the scalp, because the representations of each finger in BA3b and BA1 lie very close to each other (e.g., Fig. 2 in Holmes and Tamè 2019). We answered the question in four ways: *1*) by reanalyzing fMRI data from our laboratory (Tamè and Holmes 2016); *2*) by creating a probabilistic atlas of the central sulcus from 100 structural MRIs, and measuring between-participant variability in central sulcus location at the likely position of S1-index; *3*) by conducting two experiments that systematically mapped the effect of TMS on vibrotactile discrimination performance across the scalp; and *4*) by summarizing all our available data from individual (F)MRI-neuronavigated TMS experiments targeting S1-index. Together, these independent and converging lines of evidence strongly support the immediate revision of the most commonly used heuristic for locating human primary somatosensory cortex in TMS studies.

MATERIALS AND METHODS

Studies were approved by research ethics committees (UREC11/58, University of Reading, Reading, UK; SoPEC916, University of Nottingham, Nottingham, UK), conducted in accordance with TMS safety guidelines (Rossi et al. 2009) and the Declaration of Helsinki (2008 version, which does not require preregistration).

Participants. The fMRI experiment included 20 healthy participants (mean ± SD age = 27.6 ± 8.7 yr, 15 female, 3 left handed by self-report). The structural MRI experiment used 100 right-handed participants (mean ± SD age = 25.1 ± 6.2 yr, 64 female; Holmes et al. 2008; Tamè and Holmes 2016; Holmes NP, unpublished data sets). There were nine participants (mean ± SD age = 33.2 ± 11.6 yr, 5 female, 1 ambidextrous; 13 were recruited, 4 were removed) in *experiment 1* and 12 (mean ± SD age = 23.7 ± 5.6 yr, 5 female, 12 right handed) in *experiment 2*. Participants met TMS safety inclusion criteria (Rossi et al. 2009), with no neuropsychiatric disorder. For neuronavigation we used 37 localizations of S1-index from 15 participants, separately for left (*N* = 11, mean ± SD = 25.4 ± 6.1 yr, 7 female) and right hemispheres (*N* = 9, mean ± SD = 26.2 ± 6.3 yr, 3 female).

Functional MRI data. Data reported by Tamè and Holmes (2016) were reanalyzed. Participants underwent 10 × 280-s scans, each comprising 10 × 11.5-s vibrotactile stimulation blocks interleaved with 10 × 12.5-s rest. Stimuli were produced by MRI-compatible piezoelectric wafers driving a 2.5-mm-diameter plastic rod (~100 Hz, 8 × 1 s, 0.5-s pause). One scan (Siemens Trio 3T, 3 × 3 × 3 mm) was collected for each digit on each hand, in pseudorandomized order. fMRI data were processed with FSL5 (https://www.fMRIb.ox.ac.uk/fsl): 3D spatial smoothing [5 mm full width at half maximum (FWHM)], 6- and 12-degree-of-freedom linear registration to the anatomical [magnetization prepared rapid acquisition gradient echo (MPRAGE), 1 × 1 × 1 mm] and Montreal Neurological Institute (MNI)152 (2 × 2 × 2 mm) template brains, respectively. Data were modeled as square-wave regressors convolved with canonical hemodynamic response functions. Two contrasts were made with each set of 10 scans: single digit contrasts of vibration vs. rest, within scans; differential contrasts of each digit against the other four of that hand, across scans (e.g., left index finger (D2) contrasted against the left thumb (D1), middle (D3), ring (D4), and little (D5) digits, weights: [−1,4,−1,−1,−1]). Group means were calculated for each digit and each contrast (20 group-level images). The voxel with maximum *Z*-score in postcentral gyrus of presumed primary somatosensory cortex of each group image was recorded. Harvard-Oxford and Juelich atlases (Eickhoff et al. 2005) within FSLView were used to assign probabilistic anatomical and functional labels to voxels.

Probabilistic atlas of the central sulcus, and S1-index scalp location. Structural MRI scans were used to create a probabilistic central sulcus atlas. The location of S1-index on the scalp was estimated by measuring seven points along the scalp between midline and the scalp overlying S1-index [MNI(−48,−21,50); Holmes and Tamè 2019]. One hundred twelve scans (MPRAGE, 1 × 1 × 1 mm) were acquired from Siemens Sonata 1.5T (*N* = 43, University of Oxford); Siemens Magnetom Trio 3T (*N* = 20, University of Reading); and Philips Achieva 3T (*N* = 49, University of Nottingham). Eight were excluded for self-reported left-handedness, 1 for scan quality (artifacts), and 1 for poor health (severe uncorrected visual deficits). Two scans that did not include the full scalp, nasion, and inion were also removed.

Each image was viewed in axial/transverse plane, by N. P. Holmes or S. Zeni. Using a 2-mm "pencil," the complete bilateral course of the central sulcus was drawn on the image, starting at the hand knob, moving superiorly then inferiorly and laterally from the hand area. We filled all gaps between pre- and postcentral gyri to provide a liberal estimate of central sulcus location and width. Five landmarks were drawn on the images with 3 × 3 × 3 mm masks: nasion, inion, left and right preauricular points, vertex (Fig. 1*H*). Nasion and preauricular points were easily identified, but inion prominence varied greatly. Vertex was estimated by calculating a line orthogonal to and through the intersection of nasion-inion and preauricular lines, then using ruler and protractor to find the scalp location 90° from the intersection. A best guess for vertex location was then taken, considering three image planes. It is not known how these locations correspond to those measured on participants' heads during S1-index TMS.

Participants' brain images were extracted using FSL5's brain extraction tool (BET), and both head and brain were registered to MNI152 1 × 1 × 1-mm templates using FMRIB's Linear Image Registration Tool (FLIRT) (12 degrees of freedom). The two transformations (head, brain) were applied to central sulcus mask images to create masks in standard MNI space. One hundred masks were summed to create a probabilistic atlas of the central sulcus where voxel intensity is the percentage of participants with central sulcus passing through.

S1-index location was estimated relative to vertex using a mask of meta-analytic mean MNI coordinates for S1-index [MNI(−48,−21,50)], transformed into scanner/anatomical space per MRI. To account for nonalignment between head and scanner axes, nasion, inion, and vertex on each image were used to form a plane termed NIV (i.e., midsagittal). The nearest voxel to S1-index on the scalp was estimated and projected orthogonally onto NIV. This projection was used to generate six pairs of coordinates (*x,y*) between S1-index and NIV. Each pair's *Z*-coordinate was recorded as the most superior scalp voxel where *x*- and *y*-coordinates matched the projection. Distances between adjacent points and the distance between S1-index and vertex were calculated. For anterior distances, the *y*-coordinate of the S1-index projection onto NIV was subtracted from the vertex *y*-coordinate and divided by the cosine of the angle between nasion-inion and scanner *y*-axis.

Experiment 1: Mapping effects of TMS on tactile discrimination thresholds. Participants trained to detect and discriminate vibrotactile stimuli (150 Hz, 50 ms, Oticon bone-conductor) on their right index finger. The first training was 48 trials of two-interval forced choice (2IFC) detection, in which a pseudorandom interval contained a target. 1-s intervals were preceded by a 250-ms light-emitting diode (LED) flash on the left (first) or right (second interval). Targets were presented midinterval and were followed by a 2.5-s response period. Participants released a pedal under their left (indicating the target was in the first) or right foot (second interval). Incorrect responses were followed by 2 × 250-ms flashes from both LEDs. Trials were separated by 1 s. Target intensity began at 0.8 (arbitrary units), adjusted by QUEST (Watson and Pelli 1983) implemented in PsychToolBox3 (Brainard 1997). The second training was 2IFC intensity discrimination. One interval contained a "weak" (1.5 × detection threshold), the other a "strong" vibration (starting at 1.8 × weak intensity). Partici-
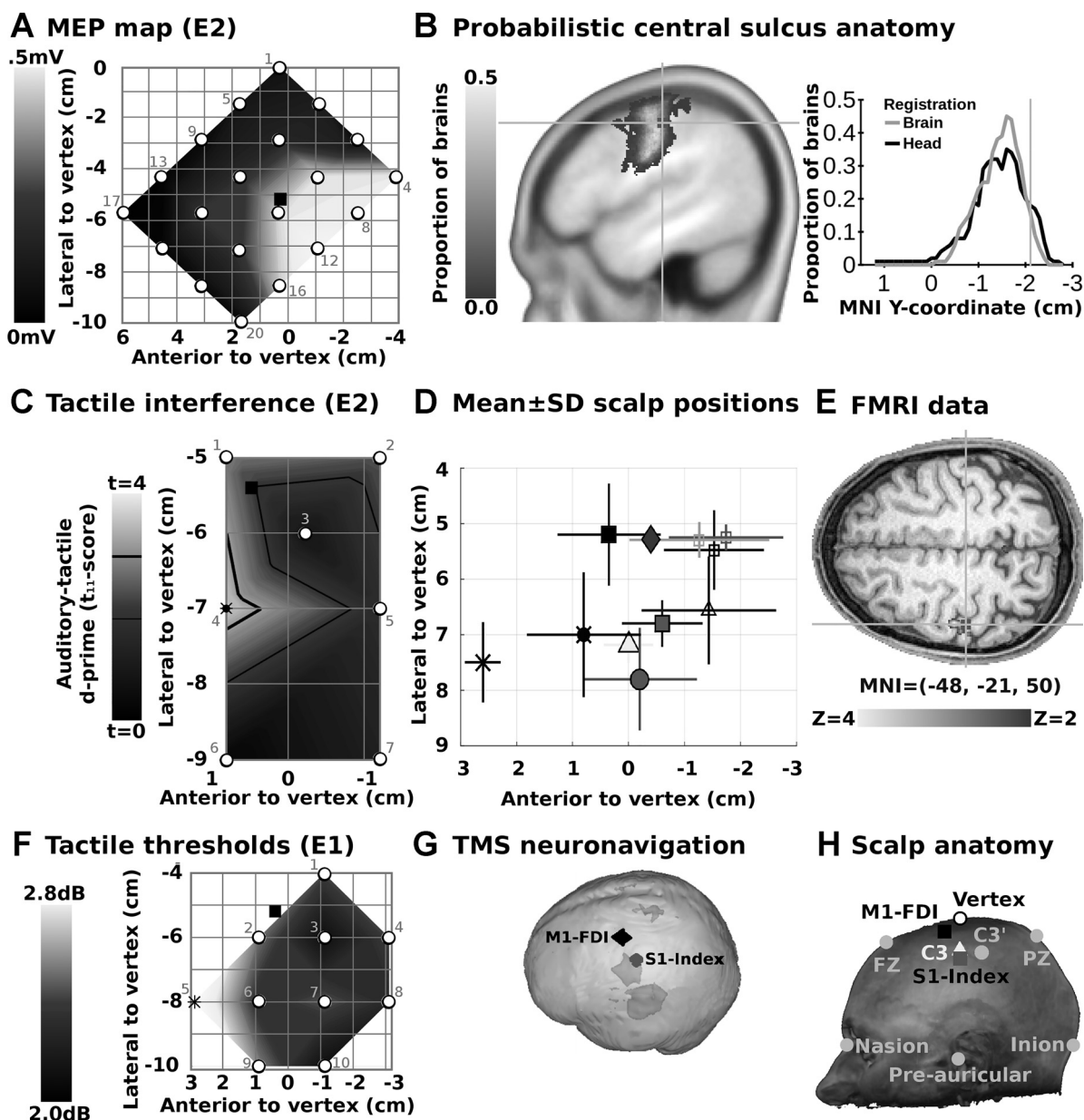
Fig. 1. Locating primary somatosensory cortex in human brain stimulation studies. Evidence for the scalp location of the primary somatosensory cortex representation of the right index finger (S1-index). All coordinates are in centimeters (cm) lateral to (i.e., left of) and anterior to (i.e., forward of) the vertex (Cz), or in Montreal Neurological Institute (MNI) space. Color available at https://osf.io/c8nhj. *A*: mean motor evoked potential (MEP) amplitude during systematic mapping of the first dorsal interosseus muscle's primary motor cortex representation (M1-FDI) on the scalp in *experiment 2*. Black square at Cz($-5.2,0.4$): mean location of M1-FDI from all available studies conducted in the laboratory ($N = 56$); white circles: locations tested. *B*: probabilistic anatomy of the central sulcus, as estimated from 100 MRI scans. Shading on the brain scan represent the proportion of participants with central sulcus at that location. Dark gray square and cross-hairs: mean reported MNI coordinate for the location of S1-index across 54 functional MRI (fMRI) studies, MNI($-48,-21,50$). The graph shows a cross-section along the MNI *y*-axis for the selected coordinate. The range of likely central sulcus distances along this axis, after transformation of either the whole head (black), or the brain (gray), is 2–3 cm. *C*: transcranial magnetic stimulation (TMS)-related interference with tactile intensity discrimination in *experiment 2* (E2) [$N = 12$, Auditory d' – Tactile d', $t(11)$-scores] is highest 7 cm lateral and 0.76 cm anterior to the vertex. Thin black contour: uncorrected 1-tailed statistical significance (alpha) threshold ($P \leq 0.05$); thick black contour: alpha threshold Bonferroni corrected for 7 locations ($P \leq 0.007$); black "target": maximum tactile interference; square: M1-FDI; white circles: locations tested. *D*: summary of all scalp locations (mean ± SD) studied in this report and those from a recent systematic review. Circle: S1-index based on individual fMRI-guided TMS neuronavigation; large triangle: mean C3 location on 101 participants' heads; open squares: estimated mean scalp location targeted for 43 TMS studies using M1-FDI as a reference point (black); 16 TMS studies using M1-thenar as a reference point (mid gray); 21 TMS studies using hand movement as a reference point (light gray); small triangle: estimated mean scalp location targeted for 16 TMS studies using C3 as a reference point; diamond: estimated mean scalp location of M1-FDI according to a meta-analysis. Black cross: mean location of maximum intensity discrimination thresholds in *experiment 1*; black target: mean location of maximum difference between auditory and tactile intensity discrimination performance in *experiment 2*. *E*: fMRI data. Reanalysis of fMRI data from Tamè and Holmes (2016): shading shows the contrast between the right index finger versus all other fingers on the right hand. *F*: mean tactile intensity discrimination thresholds for 9 participants in *experiment 1* (E1). White circles: locations tested. *G*: mean ± 95% confidence ellipsoids for M1-FDI (superior) and S1-index (inferior) locations, as used by Tamè and Holmes (2016). TMS, transcranial magnetic stimulation. *H*: scalp landmarks used in the 10-20 electrode positioning system. White circle: vertex; light gray circles: other scalp landmarks and electrode positions, including C3′, often positioned as indicated, at 2 cm posterior to C3, though likely located ~3.6 cm posterior to C3.

pants responded with left feet for strong (targets) in the first and right for the second interval. Threshold for 2IFC tasks was ~76% correct, taken as the final trial's value of QUESTMean. The third training was one-interval forced choice (1IFC) intensity discrimination. Half the intervals contained a weak ($1.5 \times$ detection threshold), and half a strong vibration (starting at $1.8 \times$ weak intensity). Participants classified stimuli as strong (left) or weak (right pedal). The strong intensity was adjusted with QUEST. Threshold was 69% correct (equivalent to 76% in 2IFC). A single pulse of TMS at 50% maximum stimulator output (MSO) was presented ~30 cm away from the participant's head, 25 ms after the onset of each vibration.

We refer to scalp and brain coordinates thus: ORIGIN(lateral, anterior). Right and anterior are positive, left and posterior negative. For example, 5 cm left and 1 cm anterior to vertex: Cz($-5,1$); 2 cm posterior to the optimal FDI location: FDI($0,-2$). MNI neuroimaging coordinates are MNI(X,Y,Z), in millimeters. Resting motor threshold (RMT) for the FDI was estimated using motor evoked potentials (MEPs) in the electromyograph (EMG, AD Instruments PowerLab 16/30; BioAmplifier, silver/silver-chloride electrodes over FDI belly and distal second metacarpal, Criswell 2011; monophasic Magstim 200^2 BiStim module, standard BiStim mode, figure-of-8, 100-mm-outer-diameter coil). Test pulses ~5–10 s apart were presented while the coil was moved around, at approximately Cz($-5,1$), starting at 50% MSO, increasing and decreasing to find the threshold (i.e., 5/10 trials with minimum peak-to-peak MEP amplitude of 50 μV, both peaks within 20–60 ms). The coil handle pointed posterolaterally, ~45° to the midline; current anterior-to-posterior.

The mapping experiment was 10 blocks of 48 trials of 1IFC intensity discrimination, with TMS at one of 10 pseudorandomly ordered locations (Fig. 1F). A grid of 10 locations was placed on participants' heads, with the origin, *location 2* (L2) = FDI($0,0$). The 9 other locations were L1 = FDI($+2,-2$), L3 = FDI($0,-2$), L4 = FDI($0,-4$), L5 = FDI($-2,+2$), L6 = FDI($-2,0$), L7 = FDI($-2,-2$), L8 = FDI($-2,-4$), L9 = FDI($-4,0$), and L10 = FDI($-4,-2$).

Two participants (*participants 3* and *8*) could not perform training. Two (*participants 10* and *12*) performed poorly with TMS (i.e., floor effects, QUEST reached ceiling) on eight blocks. *Participant 7* showed floor effects on six, *participant 11* on two, and *participants 5, 6*, and *9* on one block each. Floor effects reduce variability at lower performance ranges (Holmes 2009). A scatterplot of participants' across-block means against across-block SDs revealed two outliers (*participants 10* and *12*), with low coefficient of variation (SD/mean). These participants were removed; the reported mean effects of TMS are therefore likely underestimated.

Experiment 2: Controlling for nonspecific effects of TMS. *Experiment 1* contained one task and 10 locations. Changes in performance across locations could be due to differences in TMS-related discomfort rather than effects on the brain (Holmes and Meteyard 2018; Meteyard and Holmes 2018; http://tms-smart.info). *Experiment 2* improved TMS localization and participant performance. Participants also performed auditory intensity discrimination to control for nonspecific TMS effects.

EMG data were recorded from electrodes over FDI and flexor digitorum superficialis (FDS; Criswell 2011). M1 was systematically mapped at 20 grid locations oriented ~45° to midline (Fig. 1A). During discrimination, seven TMS locations were stimulated (4×2 grid, 2-cm spacing). An extra location was added, at FDI($-1,-1$), as our best guess (at the time) of optimal S1-index location: L1 = FDI($0,0$), L2 = FDI($0,-2$), L3 = FDI($-1,-1$), L4 = FDI($-2,0$), L5 = FDI($-2,-2$), L6 = FDI($-4,0$), and L7 = FDI($-4,-2$); see Fig. 1C. Participants performed two counterbalanced 1IFC intensity discrimination tasks (vibrotactile, auditory). In auditory blocks, a speaker was positioned near participants' hands. Target frequency was 200 Hz. Weak intensity was $2 \times$ detection threshold, strong $1.5 \times$ discrimination threshold above the weak intensity. Twenty trials with fixed intensity were used. Based on Holmes NP, unpublished data, TMS was triggered 50 ms after stimulus

onset (i.e., approximately midway through stimulus processing, assuming ~25-ms conduction time). A 75-mm outer diameter TMS coil was used.

Participants' heads were measured. Five pulses of TMS were presented at each of 20 locations on the 5 (medial-lateral) $\times$ 4 (anterior-posterior) grid (Fig. 1A), with 1-cm spacing, centered on Cz($-5,1$). The mean MEP amplitude across five pulses at each location was recorded. The 20 locations were tested sequentially, starting anteromedially, *location 1*, Cz($-3,2.5$), proceeding posterolaterally to *location 4*, Cz($-3,-0.5$), then *location 5*, Cz($-4,2.5$), finishing at *location 20*, Cz($-7,-0.5$). The location with maximal mean MEP amplitude per participant was designated M1-FDI; RMT was measured here.

Participants performed tactile and auditory tasks in two counterbalanced ~60-min sessions. Two training tasks were performed per session: 2IFC detection, 2IFC intensity discrimination. The experiment included seven blocks of 20 trials, each block with TMS over one pseudorandomized location. Data were analyzed as proportion correct, $d' = Z(\text{Hits}) - Z(\text{False alarms})$, and criterion $= -0.5 * [Z(\text{Hits}) + Z(\text{False alarms})]$ (Tamè and Holmes 2016). The coil was held at ~45° to midline, handle posterolaterally, current anterior-to-posterior.

Scalp measurements of S1-index. The scalp locations of S1-index across all our available neuronavigated TMS data from nine unpublished experiments were summarized. For all measurements we had a recent structural MRI scan and used atlas coordinates derived either from individual fMRI data, from group ($N = 20$) fMRI data, or from meta-analysis (Holmes and Tamè 2019). All available sources of information were used. The target was on the anterior bank and/or crown of postcentral gyrus. Anatomical criteria (i.e., over postcentral gyrus, posterior to central sulcus) were prioritized over fMRI data. fMRI coordinates, whether based on individual, group, or meta-analysis, indicated that S1-index was, in every participant, lateral to or on the lateral border of the precentral gyrus "hand knob" (Yousry et al. 1997).

Analytic strategy. This report provides multiple independent estimates of the optimal scalp location to stimulate S1-index. The analysis was largely exploratory, to estimate rather than hypothesis test. Means and SDs are given for distances, locations, and TMS parameters; means and standard errors (SE) are given for behavioral performance, muscle responses, and between condition differences, where statistical comparisons are made. Our experimental question is: Are there consistencies in optimal TMS location across the samples typically used in similar TMS experiments ($N \approx 12$)? Reported *P*-values are uncorrected, unless otherwise stated. We believe minimizing sample size is important for human brain stimulation experiments, to reduce the risk that TMS poses; three of our participants have suffered syncope or fainting (Reader et al. 2017). Our approach is therefore to search for large, consistent effects (Smith and Little 2018) and accumulate multiple, independent, converging sources of evidence. Where statistical tests are used, we are comfortable with the conventional long-run false positive error rate of 5% (Lakens et al. 2018). Data, scripts, and previous versions of our work are freely available at https://osf.io/c8nhj/.

RESULTS AND STATISTICAL ANALYSES

Functional MRI data. The group peak voxel locations and probabilistic anatomy for blood oxygen level-dependent (BOLD) responses to vibrotactile stimulation of 10 digits are in Table 1. The data are unable to resolve different S1 subregions, so only peak S1 voxels are reported. The differential contrasts, of each digit against the other four, resulted in lower BOLD Z-scores (across-digit mean $\pm$ SD $Z = 2.69 \pm 0.86$) than single condition contrasts (mean $\pm$ SD $Z = 4.14 \pm 0.65$), as expected — the single contrasts do not account for general task-related or finger nonspecific activity common to all conditions in contrast with rest. The peak voxels in the two

Table 1. *Peak BOLD signal changes at the group level, to vibrotactile stimulation of left and right digits in 20 healthy participants*

Hand	Contrast	Digit	MNI			Z	Central gyri		Probabilistic Anatomy, % Brodmann's area					
			x	y	z		Pre	Post	6	4a	4p	3b	1	2
Left	Differential	1	56	−12	46	3.43	20	57	9	41	1	32	82	17
		2	**48**	**−12**	**54**	**3.77**	**42**	**27**	**47**	**38**	**0**	**8**	**43**	**0**
		3	42	−20	54	2.41	32	32	15	41	13	66	19	0
		4	42	−22	62	2.83	28	34	49	38	0	21	55	0
		5	40	−30	64	1.34	5	47	7	35	8	31	76	0
	Single	1	56	−12	48	5.32	19	52	7	44	0	22	76	10
		2	**50**	**−14**	**56**	**4.39**	**17**	**50**	**26**	**18**	**0**	**0**	**37**	**0**
		3	46	−22	60	4.08	9	48	9	10	0	19	96	3
		4	40	−30	66	4.1	5	58	14	38	6	12	65	0
		5	40	−30	64	3.36	5	47	7	35	8	31	76	0
Right	Differential	1	−50	−18	44	3.34	13	51	0	20	15	44	48	60
		2	**−48**	**−14**	**50**	**3.55**	**35**	**37**	**33**	**45**	**1**	**31**	**48**	**6**
		3	−42	−20	62	2.79	38	28	60	28	0	7	32	0
		4	−44	−28	64	1.56	2	63	0	6	0	16	80	8
		5	−46	−28	62	1.92	0	62	0	2	0	11	94	19
	Single	1	−50	−20	44	4.42	6	51	0	9	11	43	50	72
		2	**−54**	**−22**	**52**	**4.80**	**0**	**69**	**0**	**0**	**0**	**8**	**88**	**30**
		3	−44	−20	62	4.17	24	41	48	19	0	5	32	0
		4	−52	−26	56	3.28	0	57	0	0	0	0	86	26
		5	−40	−30	64	3.44	5	49	2	40	0	15	71	8

Pre, precentral gyrus; Post, postcentral gyrus; *x*, Montreal Neurological Institute (MNI) *x*-coordinate (in mm); *y*, MNI *y*-coordinate (in mm); *z*, MNI *z*-coordinate (in mm); Z, Z-score for the blood oxygen level-dependent (BOLD) contrast. Probabilistic anatomy based on the Juelich probabilistic cytoarchitectural atlases viewed in FSL-view. Data for the index finger are highlighted in bold text.

contrasts were mean ± SD 5.44 ± 4.05 mm apart. Left hemisphere peak voxel locations ranged superiorly from MNI(−40,−30,64) for the little, to MNI(−50,−18,44) for the index; right hemisphere ranged from MNI(40,−30,66) for the ring, to MNI(56,−12,46) for the index finger. The peak differential contrast voxels for S1-index were MNI(−48,−14,50) for left, and MNI(48,−12,54) for right hemisphere.

Probabilistic atlas of the central sulcus, and S1-index scalp location. The 100 central sulcus masks were summed into a single image, indicating the percentage of participants whose central sulcus included each voxel (Fig. 1*B*, *left*). The brain registration was less variable than the head registration (Fig. 1*B*, *right*). The between-participant range in *y*-axis position of

the central sulcus at the level of S1-index, MNI(−48,−21,50), was ~2–3 cm. The mean ± SD location of S1-index projected onto the scalp was 6.8 ± 0.4 cm lateral and 0.6 ± 0.7 cm posterior to the vertex (Fig. 1, *B*, *D*, and *E*; Table 2).

Experiment 1: Mapping effects of TMS on tactile discrimination thresholds. In training, nine participants' mean ± SE 2IFC detection threshold was 0.473 ± 0.105 (arbitrary units); 2IFC discrimination threshold was 1.50 ± 0.09 times weak intensity (1.71 ± 0.26 dB, D'Amour and Harris 2014; Tamè et al. 2014); and 1IFC discrimination threshold was 1.52 ± 0.15 times weak intensity (1.64 ± 0.41 dB). Mean ± SD RMT = 44.3 ± 4.9% MSO. TMS was applied at mean ± SD = 119 ± 1.7% RMT (mean ± SD = 52.7 ± 5.3% MSO). Due to

Table 2. *Scalp locations of M1-FDI, S1-index, and C3/C4 relative to vertex (Cz), from seven independent sources of evidence*

Location and source	Location Relative to Vertex (Cz) mean ± SD cm (min:max)					
	Left hemisphere			Right hemisphere		
	N	Lateral	Anterior	N	Lateral	Anterior
M1-FDI, TMS studies (2011–2018)	56	−5.2 ± 0.8 (−7.0:-3.0)	0.4 ± 0.9 (−2.6:2.0)	14	5.2 ± 0.9 (3.5:7.5)	0.5 ± 0.9 (−1:1.8)
S1-index, TMS meta-analysis (N = 96 studies, 1991–2017)*	1693	−5.9 ± 0.9 (−8.2:-4.4)	−1.3 ± 1.0 (−3.6:0.4)			
C3/C4, head measurements (2016–2018)	101	−7.2 ± 0.3 (−7.8:-6.6)	0			
S1-index, fMRI meta-analysis (LH N = 425; RH N = 316, 54 studies, 1999–2017), projected onto scalp in MRI	100	−6.8 ± 0.4 (−9.4:-5.7)	−0.6 ± 0.7 (−2.3:2.2)	100	6.9 ± 0.4 (6.1:9.8)	−0.6 ± 0.8 (−2.3:1.8)
S1-index, *Experiment 1* (2014–2015)	10	−7.5 ± 0.7 (−9.0:-7.0)	2.6 ± 0.3 (2.0:3.0)			
S1-index, *Experiment 2* (2017)	12	−7.0 ± 1.1 (−8.8:-5.2)	0.8 ± 1.0 (−1.5:2.1)			
S1-index, fMRI study (N = 20, 2012–2014), group contrast projected onto scalp in navigated TMS studies (2016–2018)	11	−7.8 ± 0.9 (−10.0:-6.7)	−0.2 ± 1.0 (−1.5:1.4)	9	8.4 ± 1.1 (7.0:10.3)	−0.4 ± 0.6 (−1.1:0.3)

fMRI, functional magnetic resonance imaging; LH, left hemisphere; M1-FDI, first dorsal interosseus muscle's primary motor cortex representation; RH, right hemisphere; S1-index, representations of the index finger; TMS, transcranial magnetic stimulation. *Collapsed across hemispheres, and using assumed scalp locations for M1-FDI representations where not reported.

researchers not recording data, scalp locations for M1-FDI were available for only seven participants, with mean ± SD Cz(6.0 ± 1.0,0.9 ± 0.6) cm. Overall mean ± SE discrimination threshold across 10 locations was 2.73 ± 0.26 dB (Fig. 1*F*), with best performance (2.3 ± 0.4 dB) at FDI(0,−2), and worst (3.36 ± 0.31 dB) at FDI(−2,2) (Fig. 1, *D* and *F*). Thresholds were higher (worse) than in training, with *locations 5*, *6*, and *9* significantly different (0.012 ≤ P ≤ 0.032). Pairwise comparisons between all 10 sites revealed significant differences between FDI(−2,2), and *locations 2*, *3*, *4*, *6*, *8*, and *10* (0.026 ≤ P ≤ 0.049). Across locations, mean ± SE MEPs were 0.178 ± 0.039 mV, from 0.106 ± 0.027 mV at FDI(0,−4), to 0.439 ± 0.186 mV at FDI(0,0). Within-participant correlations between MEP amplitude and discrimination threshold across 10 locations varied from $r(8) = -0.499$ to $r(8) = 0.417$ (uncorrected two-tailed ps > 0.14). R-values were converted to Z-scores to allow parametric analysis; across participants, mean ± SE Z-score was small (0.100 ± 0.110, $t(8) = 0.905$, $P = 0.389$).

Experiment 2: Controlling for nonspecific effects of TMS. Training performance on 2IFC detection was mean ± SE = 0.0483 ± 0.0112 (arbitrary units) for tactile, and 0.0319 ± 0.0029 for auditory stimuli, $t(11) = 0.145$, $P = 0.887$. 2IFC intensity discrimination performance was 0.352 ± 0.055 (1.27 ± 0.16 dB) for tactile, and 0.524 ± 0.113 (1.71 ± 0.30 dB) for auditory, $t(11) = 0.876$, $P = 0.160$. Participants' head sizes were a mean ± SD = 38.0 ± 2.3 cm from nasion-inion, and 36.5 ± 1.8 cm between preauricular points. Across locations, mean ± SE MEP amplitude = 0.197 ± 0.056 mV, from 0.003 ± 0.002 mV at Cz(−5.4,3.5), to 0.526 ± 0.283 mV at Cz(−6.1,−0.1) (Fig. 1*A*). *Locations 3*, *6*, *9–11*, and *15* produced MEPs significantly greater than zero (0.005 ≤ P ≤ 0.020). Pairwise comparisons revealed no clear pattern of differences. Across participants, Cz(−4.7,−1.5), Cz(−3.9,2.1), Cz(−4.7,1.4), Cz(−5.4,2.1), and Cz(−6.8,0.7) produced maximal MEPs in one participant, Cz(−3.2,1.4) and Cz(−6.1,−0.1) in two, and Cz(−5.4,0.7) in three. Mean ± SD optimal location was Cz(−5.0 ± 1.1,0.8 ± 1.0). Mean ± SD RMT at this site was 40.4 ± 7.0%MSO.

TMS was presented during the experiment at a mean ± SD of 120 ± 0.6% RMT (48.4 ± 8.4% MSO). Performance was worse with tactile (mean ± SE $d' = 1.06 ± 0.12$) than auditory targets [1.61 ± 0.2, $t(11) = 2.78$, $P = 0.018$]. Response biases (tendency to respond "stronger") were negligible, and comparable between touch (mean ± SE criterion = −0.005 ± 0.039) and audition [0.055 ± 0.054, $t(11) = 0.938$, $P = 0.369$]. Effects of TMS were assessed by differences between auditory and tactile tasks per location. TMS over FDI(−2,0) resulted in the largest decrement in performance [tactile mean ± SE $d' = 1.05 ± 0.30$ vs. auditory = 1.93 ± 0.30, mean ± SE difference = 0.880 ± 0.265, $t(11) = 3.32$, $P = 0.007$], with FDI(0,0) second largest [0.942 ± 0.194 vs. 1.73 ± 0.346, difference = 0.788 ± 0.318, $t(11) = 2.48$, $P = 0.031$, Fig. 1, *C* and *D*; Table 2]. All other sites showed worse performance for tactile targets, but none significantly. None of the response biases differed between auditory and tactile tasks, but participants were more likely to report "weaker" tactile targets with TMS over FDI(0,0) (mean ± SE criterion = −0.136 ± 0.075), than FDI(−2,0) [0.120 ± 0.087, $t(11) = 2.39$, $P = 0.036$], or FDI(−2,−2) [0.130 ± 0.110, $t(11) = 2.26$, $P = 0.045$].

MEPs were recorded from FDI and FDS and were monitored during experiments, but data were saved only for eight participants (*participants 5–12*). During the tactile task, mean ± SE

MEPs were smallest at FDI(−4,0) (FDI = 0.058 ± 0.026 mV) and FDI(−2,−2) (FDS = 0.014 ± 0.010 mV) and largest at FDI(0,0) (FDI = 1.51 ± 0.49 mV, FDS = 1.22 ± 0.43 mV). During the auditory task, MEPs were smallest at FDI(−2,−2) (FDI = 0.01 ± 0.01 mV; FDS = 0.01 ± 0.01 mV) and largest at FDI(0,0) (FDI = 0.79 ± 0.29 mV, FDS = 0.55 ± 0.21 mV). The smallest MEPs (~0.01 mV) were not different from zero, much lower than the MEP threshold, and likely reflect electrical noise. Comparing auditory and tactile tasks, MEPs were not significantly different at any location. There were no significant correlations between performance (d') and MEP amplitude, either for tactile or auditory tasks alone, the differences between them, for either muscle, or for both muscles combined [nine comparisons on Z-scores, all $t(7) ≤ 1.75$, all uncorrected $P ≥ 0.125$].

Scalp measurements of S1-index. The mean ± SD scalp location of S1-index was Cz(−8.0 ± 0.9,−0.4 ± 1.0) (left hemisphere, Fig. 1*D*; Table 2), and Cz(8.4 ± 1.1,−0.4 ± 0.5) (right hemisphere). Combining hemispheres across 15 participants, S1-index was at Cz(±8.1 ± 1.0,−0.3 ± 0.8). For seven participants, mean ± SD S1-index was at FDI(±2.4 ± 1.0,−0.5 ± 1.3).

DISCUSSION

Reanalysis of fMRI data revealed the peak voxel for right index finger was very close to the meta-analytic mean location of S1-index in BA3b and BA1. The probabilistic central sulcus atlas revealed a 2–3 cm anterior-posterior range in central sulcus location at the level of S1-index. This implies that researchers using template MRI to position TMS coils are likely to make *y*-axis errors of several centimeters in locating the central sulcus. Projected onto the scalp, S1-index is 7 cm lateral and 0.5 cm posterior to vertex. These distances are likely to be slight underestimates, given that participants typically have hair (not visible on MRI), and a bathing or EEG cap between scalp and TMS coil. This underestimation is between 0.2 and 1.0 cm (Table 2). In *experiment 1*, the location of maximal interference of TMS with tactile intensity discrimination thresholds was 2 cm lateral, and 2 cm anterior to M1-FDI. *Experiment 1*, however, is relatively weak: two participants could not complete the task, two were removed, and the statistical tests did not pass conservative multiple comparison corrections. Instead, *experiment 2* provides strong evidence that maximal interference with tactile intensity discrimination is 2 cm lateral to M1-FDI. *Experiment 2* allows greater confidence that M1-FDI was optimally localized and that tactile interference was due to a specific worsening of tactile relative to auditory discrimination. Conservative correction for multiple comparisons revealed that the only significant effect of TMS on tactile intensity discrimination was 2 cm lateral to M1-FDI.

The more anterior location found in *experiment 1* than *2* may be due to the different tasks used (threshold estimation vs. discrimination); to between-participant differences in central sulcus anatomy or head shape; to variability in the precision of our TMS methods and head measurements; or to increased TMS-related discomfort at the most anterior site in *experiment 1* (Holmes and Meteyard 2018; Meteyard and Holmes 2018). *Experiment 2* included a control task so that TMS-related discomfort was matched, and task-related differences were the

dependent variable. Without independent MRI evidence, the most likely cause is measurement error and increased TMS-related discomfort at the most anterior site in *experiment 1*.

Here, we reported multiple independent lines of evidence (Table 2, Fig. 1) which supports findings from a recent systematic review (Holmes and Tamè 2019): the optimal location for stimulating the hand area of primary somatosensory cortex, on average, is ~2 cm lateral and ~0.5 cm posterior to M1-FDI. This finding of S1-hand being more lateral than M1-hand is consistent with studies in which both M1-hand and S1-hand are measured together (e.g., Blatow et al. 2011), and with the work of Seyal and colleagues (1997), who systematically mapped TMS effects on tactile detection and discrimination at 25 locations in a grid centered on M1-hand. They found maximal interference when the TMS coil was 4 cm lateral and 0–2 cm posterior to M1-hand (Fig. 2, *a* and *b* in Seyal et al. 1997).

Assuming previous TMS studies found M1-FDI/APB in a similar location to our data, these results imply that TMS studies targeting S1-index have been, on average, 2.25 cm away from their target (Table 1). This is not a trivial distance. The mean figure-of-8 TMS coil used in these studies has a 7.5-cm outer wing diameter, implying an error of 30% of coil diameter. This is likely to impede stimulation effectiveness. TMS over motor cortex is sensitive to coil position changes of a few millimeters (e.g., Raffin et al. 2015). These large distances between the likely location of S1-index, and the locations targeted in prior experiments may explain why otherwise well-designed experiments may fail to interfere significantly with tactile perception (e.g., Convento et al. 2018, reviewed by Holmes and Tamè 2018). Below, we discuss possible sources of variability in stimulating S1 using TMS.

Sources of variability in stimulating S1. Variability in TMS studies arises from participants, experimenters, and procedures. Participant-associated variability includes head size and shape (Xiao et al. 2018; Zilles et al. 2001), brain area size, shape, folding, location, and function. Experimenter-associated variability arises from the selection, measurement, and registration of anatomical landmarks and reference points (nasion, inion, vertex), and the positioning and orientation of the coil. Procedure-associated variability includes the target, timing, intensity, orientation, waveform, frequency, and orientation of TMS.

We were surprised by the large within-participant and between-session/experimenter variability during our studies. This variability may explain the potentially surprising finding of *experiment 1*, with maximal thresholds 2 cm lateral and 2 cm anterior to M1-FDI. Measurements on the scalp varied, laterally and anteriorly, by 3–4 cm between participants for M1-FDI relative to vertex (Niskanen et al. 2010), S1-index relative to vertex, and S1-index relative to M1-FDI. In part, this is due to errors in scalp measurement, MRI registration, and locating M1-FDI. In large part, however, it likely reflects between-participant anatomical differences. Better training, communication, and day-to-day practice will minimize experimenter error; better understanding of M1-hand and S1-hand is required to optimize TMS protocols. Given the potential sources of variability in stimulating S1, we recommend consistent, systematic, and numerical reporting of every aspect and stage of TMS studies (Chipchase et al. 2012; Rossi et al. 2009; Rossini et al. 1994, 2015). This should be done for all studies, regardless of whether neuronavigation was used.

Limitations. Our approach relied on numerous sources of information which, we argued, converged on the result that S1-index is 2 cm lateral to M1-FDI. Despite this convergence, one might question whether meta-analysis of reported fMRI coordinates, or averaging fMRI data across participants is sufficient. We cannot distinguish between Brodmann's area BA3b, BA1, or BA2 with our fMRI data, as our localizers were not sufficiently powerful. Similar limitations may apply to our TMS data (Fox et al. 2004). We also cannot account for biases intrinsic to fMRI — the data rely on oxygenation changes rather than neural activity and may be biased by nonneural structures (Schweisfurth et al. 2014). Furthermore, single peak voxel coordinates derived from multiple studies and participants do not reflect the likely extent of S1 activation following index finger stimulation, nor the total S1 territory involved. Better methods to estimate the optimal scalp location for S1-index TMS may be to combine probabilistic maps of S1 with the likelihood of effective TMS, accounting for individual brain anatomy (Petrov et al. 2017). The overlap or convolution of these probabilistic maps might provide more accurate estimates of the scalp locations necessary to stimulate S1-index. This approach represents a clear goal for future work and would be extremely useful for interpreting previous results and planning new studies (Xiao et al. 2018). Generating such a statistic will need to account for TMS coil size, shape, position, and orientation; TMS pulse intensity, waveform, frequency, and pattern; scalp-to-brain distance; cortical folding; and the size and function of the cortical area under study.

We have criticized the standard heuristic based on M1-FDI to locate S1-index, but our methods also rely on TMS over M1-FDI: the origin of our maps was M1-FDI; TMS intensity was set according to M1-FDI threshold. These practices are very common in TMS research, but we must be cautious about the circularity. There may be no reason why S1-index is best localized using M1-FDI as a reference and no reason why parameters optimal for M1-FDI should be optimal for S1-index. Addressing this circularity is outside the present scope but is important for future studies.

Recommendations for locating S1-index in transcranial stimulation studies. Depending on available equipment and funding, transcranial stimulation studies may need different methods to locate their targets. Ideally, neuronavigation with a recent high-resolution structural MRI and functional localizer will be used for each participant. Systematic review showed that very few studies met this gold standard (Holmes and Tamè 2019). If individual fMRI is unavailable, individual MRI with group-level localizers or coordinates may suffice. The fMRI data need to be interpreted in conjunction with anatomical criteria. Registration of the participant's head to the MRI needs to be done carefully; we recommend recording head and scalp measurements systematically — in one participant, we noticed scalp coordinates well outside other participants'; reregistering the MRI revealed that the wrong calibration file had been used, leading to ~3-cm coil positioning error. If a participant's MRI is unavailable, then standard MRI templates, registered onto the participant's scalp, provide only an approximate localization. The probabilistic central sulcus atlas we reported (Fig. 1*B*), suggests registration errors of several centimeters are likely. Without neuronavigation, scalp measurements using the 10-20 or 10-10 systems may be the only, very approximate, localization method. If the location of a target is estimated

relative to that of primary motor cortex (i.e., using muscle twitches or MEPs), or other functionally defined locations, then researchers should use as many relevant sources of evidence to justify any heuristics used. Our work suggests that even very commonly reported heuristics are not optimal for locating the intended target. Such heuristics may not be evidence based.

Conclusion. More than a century after the first electrical stimulation of human somatosensory cortex (Cushing 1909), the accuracy of TMS coil positioning remains questionable. The localization error in previous TMS studies of S1-hand is likely ~2.25 cm. Evidence from the independent sources reported here converged on the finding that S1-index is ~7–8 cm lateral to the vertex, or ~2 cm lateral and 0.5 cm posterior to the optimal scalp location for eliciting MEPs in the FDI muscle. These estimates cannot be relied upon for any single participant; the range of scalp locations across participants was 3–4 cm in each direction for each location. Multiple sources of evidence for target location — probabilistic anatomy, group data, scalp measurements, meta-analyses, and the gold standard of individual (f)MRI — should be sought in every TMS study. To improve localization methods, we recommend systematic reporting of participants' head sizes and all locations targeted, both along the scalp and, if available, in MRI scanner/anatomical and standard (e.g., MNI152) coordinates. The results of previous TMS studies targeting the index finger area of S1 need reassessment.

DISCLOSURES

No conflicts of interest, financial or otherwise, are declared by the authors.

AUTHOR CONTRIBUTIONS

N.P.H. conceived and designed research; N.P.H., L.T., P.B., M.M., M.R., and A.S. performed experiments; N.P.H., L.T., P.B., A.S., and S.Z. analyzed data; N.P.H., L.T., P.B., and A.S. interpreted results of experiments; N.P.H. prepared figures; N.P.H. drafted manuscript; N.P.H., L.T., P.B., M.M., M.R., A.S., and S.Z. edited and revised manuscript; N.P.H., L.T., P.B., M.M., M.R., A.S., and S.Z. approved final version of manuscript.

ENDNOTE

At the request of the authors, readers are herein alerted to the fact that additional materials related to this manuscript may be found at the institutional website of one of the authors, which at the time of publication they indicate is: https://osf.io/c8nhj/. These materials are not a part of this manuscript, and have not undergone peer review by the American Physiological Society (APS). APS and the journal editors take no responsibility for these materials, for the website address, or for any links to or from it.

REFERENCES

Balslev D, Christensen LOD, Lee JH, Law I, Paulson OB, Miall RC. Enhanced accuracy in novel mirror drawing after repetitive transcranial magnetic stimulation-induced proprioceptive deafferentation. *J Neurosci* 24: 9698–9702, 2004. doi:10.1523/JNEUROSCI.1738-04.2004.

Barker AT, Jalinous R, Freeston IL. Non-invasive magnetic stimulation of human motor cortex. *Lancet* 325: 1106–1107, 1985. doi:10.1016/S0140-6736(85)92413-4.

Blatow M, Reinhardt J, Riffel K, Nennig E, Wengenroth M, Stippich C. Clinical functional MRI of sensorimotor cortex using passive motor and sensory stimulation at 3 tesla. *J Magn Reson Imag* 34: 429–437, 2011. doi:10.1002/jmri.22629.

Brainard DH. The psychophysics toolbox. *Spat Vis* 10: 433–436, 1997. doi:10.1163/156856897X00357.

Chipchase L, Schabrun S, Cohen L, Hodges P, Ridding M, Rothwell J, Taylor J, Ziemann U. A checklist for assessing the methodological quality of studies using transcranial magnetic stimulation to study the motor system: an international consensus study. *Clin Neurophysiol* 123: 1698–1704, 2012. doi:10.1016/j.clinph.2012.05.003.

Convento S, Rahman MS, Yau JM. Selective attention gates the interactive crossmodal coupling between perceptual systems. *Curr Biol* 28: 746–752.e5, 2018. doi:10.1016/j.cub.2018.01.021.

Cowey A, Walsh V. Magnetically induced phosphenes in sighted, blind and blindsighted observers. *Neuroreport* 11: 3269–3273, 2000. doi:10.1097/00001756-200009280-00044.

Criswell E. *Cram's Introduction to Surface Electromyography*. London: Jones and Barlett, 2011.

Cushing H. A note upon the Faradic stimulation of the postcentral gyrus in conscious patients. *Brain* 32: 44–54, 1909. doi:10.1093/brain/32.1.44.

D'Amour S, Harris LR. Contralateral tactile masking between forearms. *Exp Brain Res* 232: 821–826, 2014. doi:10.1007/s00221-013-3791-y.

Eickhoff SB, Stephan KE, Mohlberg H, Grefkes C, Fink GR, Amunts K, Zilles K. A new SPM toolbox for combining probabilistic cytoarchitectonic maps and functional imaging data. *Neuroimage* 25: 1325–1335, 2005. doi:10.1016/j.neuroimage.2004.12.034.

Enomoto H, Ugawa Y, Hanajima R, Yuasa K, Mochizuki H, Terao Y, Shiio Y, Furubayashi T, Iwata NK, Kanazawa I. Decreased sensory cortical excitability after 1 Hz rTMS over the ipsilateral primary motor cortex. *Clin Neurophysiol* 112: 2154–2158, 2001. doi:10.1016/S1388-2457(01)00667-8.

Fox PT, Narayana S, Tandon N, Sandoval H, Fox SP, Kochunov P, Lancaster JL. Column-based model of electric field excitation of cerebral cortex. *Hum Brain Mapp* 22: 1–14, 2004. doi:10.1002/hbm.20006.

Geyer S, Schleicher A, Zilles K. Areas 3a, 3b, and 1 of human primary somatosensory cortex: Part 1. Micro structural organization and interindividual variabilities. *Neuroimage* 10: 63–83, 1999. doi:10.1006/nimg.1999.0440.

Holmes NP. The principle of inverse effectiveness in multisensory integration: some statistical considerations. *Brain Topogr* 21: 168–176, 2009. doi:10.1007/s10548-009-0097-2.

Holmes NP, Meteyard L. Subjective discomfort of TMS predicts reaction times differences in published studies. *Front Psychol* 9: 1989, 2018. doi:10.3389/fpsyg.2018.01989.

Holmes NP, Spence C, Hansen PC, Mackay CE, Calvert GA. The multisensory attentional consequences of tool use: a functional magnetic resonance imaging study. *PLoS One* 3: e3502, 2008. doi:10.1371/journal.pone.0003502.

Holmes NP, Tamè L. Multisensory perception: magnetic disruption of attention in human parietal lobe. *Curr Biol* 28: R259–R261, 2018. doi:10.1016/j.cub.2018.01.078.

Holmes NP, Tamè L. Locating primary somatosensory cortex in human brain stimulation studies: systematic review and meta-analytic evidence. *J Neurophysiol* 121: 152–162, 2019. doi:10.1152/jn.00614.2018.

Jasper H. Report of the committee on methods of clinical examination in electroencephalography: 1957. *Electroencephalogr Clin Neurophysiol* 10: 370–375, 1958. doi:10.1016/0013-4694(58)90053-1.

Koessler L, Maillard L, Benhadid A, Vignal JP, Felblinger J, Vespignani H, Braun M. Automated cortical projection of EEG sensors: anatomical correlation via the international 10-10 system. *Neuroimage* 46: 64–72, 2009. doi:10.1016/j.neuroimage.2009.02.006.

Lagerlund TD, Sharbrough FW, Jack CR Jr, Erickson BJ, Strelow DC, Cicora KM, Busacker NE. Determination of 10-20 system electrode locations using magnetic resonance image scanning with markers. *Electroencephalogr Clin Neurophysiol* 86: 7–14, 1993. doi:10.1016/0013-4694(93)90062-Z.

Lakens D, Adolfi F, Albers CJ, Anvari F, Apps MAJ, Argamon SE, Baguley T, Becker RB, Benning SD, Bradford DE, Buchanan EM, Caldwell AR, Van Calster B, Carlsson R, Chen S, Chung B, Colling LJ, Collins GS, Crook Z, Cross ES, Daniels S, Danielsson H, DeBruine LM, Dunleavy DJ, Earp BD, Feist MI, Ferrell JD, Field JG, Fox NW, Friesen A, Gomes C, Gonzalez-Marquez M, Grange JA, Grieve AP, Grist J, Guggenberger R, van Harmelen A, Hasselman F, Hochard KD, Hoffarth MR, Holmes NP, Ingre M, Isager PM, Isotalus HK, Johansson C, Juszczyk K, Kenny DA, Khalil AA, Konat B, Lao J, Larsen EG, Lodder GMA, Lukavský J, Madan CR, Manheim D, Martin SR, Martin AE,

Mayo DG, McCarthy RJ, McConway K, McFarland C, Nio A, Nilsonne G, de Oliveir CL, Orban de Xivry J, Parsons S, Pfuhl G, Quinn KA, Marmolejo-Ramos F, Sakon JJ, Saribay SA, Schneider IK, Selvaraju M, Sjoerds Z, Smith SG, Smits T, Spies J, Sreekumar V, Steltenpohl CN, Stenhouse N, Świątkowski W, Vadillo MA, van Assen MALM, Williams MN, Williams SE, Williams DR, Yarkoni T, Ziano I, Zwaan RA. Justify your alpha: a response to "Redefine statistical significance". *Nat Hum Behav* 2: 168–181, 2018. doi:10.17605/OSF.IO/9S3Y6.

Meteyard L, Holmes NP. TMS SMART — Scalp mapping of annoyance ratings and twitches caused by Transcranial Magnetic Stimulation. *J Neurosci Methods* 299: 34–44, 2018. doi:10.1016/j.jneumeth.2018.02.008.

Nelson AJ, Chen R. Digit somatotopy within cortical areas of the postcentral gyrus in humans. *Cereb Cortex* 18: 2341–2351, 2008. doi:10.1093/cercor/bhm257.

Niskanen E, Julkunen P, Säisänen L, Vanninen R, Karjalainen P, Könönen M. Group-level variations in motor representation areas of thenar and anterior tibial muscles: Navigated Transcranial Magnetic Stimulation Study. *Hum Brain Mapp* 31: 1272–1280, 2010. doi:10.1002/hbm.20942.

Okamoto M, Dan H, Sakamoto K, Takeo K, Shimizu K, Kohno S, Oda I, Isobe S, Suzuki T, Kohyama K, Dan I. Three-dimensional probabilistic anatomical cranio-cerebral correlation via the international 10-20 system oriented for transcranial functional brain mapping. *Neuroimage* 21: 99–111, 2004. doi:10.1016/j.neuroimage.2003.08.026.

Petrov PI, Mandija S, Sommer IEC, van den Berg CAT, Neggers SFW. How much detail is needed in modeling a transcranial magnetic stimulation figure-8 coil: Measurements and brain simulations. *PLoS One* 12: e0178952, 2017. doi:10.1371/journal.pone.0178952.

Raffin E, Pellegrino G, Di Lazzaro V, Thielscher A, Siebner HR. Bringing transcranial mapping into shape: sulcus-aligned mapping captures motor somatotopy in human primary motor hand area. *Neuroimage* 120: 164–175, 2015. doi:10.1016/j.neuroimage.2015.07.024.

Reader AT, Tamè L, Holmes NP. Two instances of presyncope during magnetic stimulation of the median nerve, and evaluation of resting motor threshold with transcranial magnetic stimulation (TMS). *Open Science Framework*, 9 Oct. 2017. https://osf.io/maurc/.

Rossi S, Hallett M, Rossini PM, Pascual-Leone A; Safety of TMS Consensus Group. Safety, ethical considerations, and application guidelines for the use of transcranial magnetic stimulation in clinical practice and research. *Clin Neurophysiol* 120: 2008–2039, 2009. doi:10.1016/j.clinph.2009.08.016.

Rossini PM, Barker AT, Berardelli A, Caramia MD, Caruso G, Cracco RQ, Dimitrijević MR, Hallett M, Katayama Y, Lücking CH, Maertens de Noordhout AL, Marsden CD, Murray NMF, Rothwell JC, Swash M, Tomberg C. Non-invasive electrical and magnetic stimulation of the brain, spinal cord and roots: basic principles and procedures for routine clinical application. Report of an IFCN committee. *Electroencephalogr Clin Neurophysiol* 91: 79–92, 1994. doi:10.1016/0013-4694(94)90029-9.

Rossini PM, Burke D, Chen R, Cohen LG, Daskalakis Z, Di Iorio R, Di Lazzaro V, Ferreri F, Fitzgerald PB, George MS, Hallett M, Lefaucheur JP, Langguth B, Matsumoto H, Miniussi C, Nitsche MA, Pascual-Leone A, Paulus W, Rossi S, Rothwell JC, Siebner HR, Ugawa Y, Walsh V, Ziemann U. Non-invasive electrical and magnetic stimulation of the brain, spinal cord, roots and peripheral nerves: basic principles and procedures for routine clinical and research application. An updated report from an I.F.C.N. Committee. *Clin Neurophysiol* 126: 1071–1107, 2015. doi:10.1016/j.clinph.2015.02.001.

Schweisfurth MA, Frahm J, Schweizer R. Individual fMRI maps of all phalanges and digit bases of all fingers in human primary somatosensory cortex. *Front Hum Neurosci* 8: 658, 2014. doi:10.3389/fnhum.2014.00658.

Seyal M, Siddiqui I, Hundal NS. Suppression of spatial localization of a cutaneous stimulus following transcranial magnetic pulse stimulation of the sensorimotor cortex. *Electroencephalogr Clin Neurophysiol* 105: 24–28, 1997. doi:10.1016/S0924-980X(96)96090-7.

Smith PL, Little DR. Small is beautiful: in defense of the small-*N* design. *Psychon Bull Rev* 25: 2083–2101, 2018. doi:10.3758/s13423-018-1451-8.

Sparing R, Hesse MD, Fink GR. Neuronavigation for transcranial magnetic stimulation (TMS): where we are and where we are going. *Cortex* 46: 118–120, 2010. doi:10.1016/j.cortex.2009.02.018.

Sugishita M, Takayama Y. Paraesthesia elicited by repetitive magnetic stimulation of the postcentral gyrus. *Neuroreport* 4: 569–570, 1993. doi:10.1097/00001756-199305000-00027.

Tamè L, Holmes NP. Involvement of human primary somatosensory cortex in vibrotactile detection depends on task demand. *Neuroimage* 138: 184–196, 2016. doi:10.1016/j.neuroimage.2016.05.056.

Tamè L, Moles A, Holmes NP. Within, but not between hands interactions in vibrotactile detection thresholds reflect somatosensory receptive field organization. *Front Psychol* 5: 174, 2014. doi:10.3389/fpsyg.2014.00174.

Towle VL, Bolaños J, Suarez D, Tan K, Grzeszczuk R, Levin DN, Cakmur R, Frank SA, Spire JP. The spatial location of EEG electrodes: locating the best-fitting sphere relative to cortical anatomy. *Electroencephalogr Clin Neurophysiol* 86: 1–6, 1993. doi:10.1016/0013-4694(93)90061-Y.

Vitali P, Avanzini G, Caposio L, Fallica E, Grigoletti L, Maccagnano E, Villani F. Cortical location of 10-20 system electrodes on normalized cortical MRI surfaces. *Int J Bioelectromagn* 4: 147–148, 2002.

Watson AB, Pelli DG. QUEST: a Bayesian adaptive psychometric method. *Percept Psychophys* 33: 113–120, 1983. doi:10.3758/BF03202828.

Xiao X, Yu X, Zhang Z, Zhao Y, Jiang Y, Li Z, Yang Y, Zhu C. Transcranial brain atlas. *Sci Adv* 4: eaar6904, 2018. doi:10.1126/sciadv.aar6904.

Yousry TA, Schmid UD, Alkadhi H, Schmidt D, Peraud A, Buettner A, Winkler P. Localization of the motor hand area to a knob on the precentral gyrus. A new landmark. *Brain* 120: 141–157, 1997. doi:10.1093/brain/120.1.141.

Zilles K, Kawashima R, Dabringhaus A, Fukuda H, Schormann T. Hemispheric shape of European and Japanese brains: 3-D MRI analysis of intersubject variability, ethnical, and gender differences. *Neuroimage* 13: 262–271, 2001. doi:10.1006/nimg.2000.0688.